Available online at www.sciencedirect.com
SCIENCE DIRECT®
Journal of Sound and Vibration 272 (2004) 301–316
JOURNAL OF SOUND AND VIBRATION
www.elsevier.com/locate/jsvi

# Natural frequencies of a bar with multiple cracks

R. Ruotolo[a], C. Surace[b,*]

[a] Department of Aerospace Engineering, Politecnico di Torino, Corso Duca degli Abruzzi 24, Torino, Italy
[b] Department of Structural and Geotechnical Engineering, Politecnico di Torino, Corso Duca degli Abruzzi 24, Torino, Italy

Received 14 October 2002; accepted 17 March 2003

**Abstract**

In this paper the smooth function method, previously proposed for bending vibrations, is extended to the calculation of longitudinal natural frequencies of a vibrating isotropic bar with an arbitrary finite number of symmetric transverse open cracks. Moreover, the transfer matrix approach and the finite element method are considered to deal with the same problem. The paper includes several examples related to bars with three cracks which permit the comparison of natural frequencies predicted by these three methods.


## 1. Introduction

Vibration-based inspection (VBI) is an area of active research and of great interest for future leading edge technologies such as health monitoring. A number of researchers have dealt with this topic by addressing either the direct or the inverse problem, i.e., the estimation of the effects of structural damage on the eigenparameters of the structure under study and the problem of detecting, locating and quantifying the extent of damage, respectively. A complete review of documented research in this area can be found in Ref. [1]; furthermore Dimarogonas [2] presents a state-of-the-art review of methods developed to deal with cracked structures.

In order to investigate the prevailing effects of damage present in the structure under examination, a mathematical model of the damage must be introduced into the model of the structure at the location of the fault. Different damage models have been considered. While focusing on transverse oscillations, a simple stiffness reduction of the damaged region was used in Ref. [3]. Dimarogonas [4] introduced a local flexibility model for a crack to analyse the dynamic behaviour of cracked beams and Chondros and Dimarogonas [5] combined this spring hinge

*Corresponding author. Fax: +39-011-5644899.
*E-mail address:* cecilia.surace@polito.it (C. Surace).

0022-460X/$ - see front matter 
doi:10.1016/S0022-460X(03)00761-2

model with fracture mechanics results, developing also a frequency spectral method to identify cracks in various structures. This rotational massless spring model, with stiffness related to the crack extent in the damaged section, has been used in a number of investigations [6–12]. Christides and Barr [13] developed a cracked Euler–Bernoulli beam theory by deriving the differential equation and related boundary conditions for a uniform beam with one or more pairs of symmetric cracks.

These or similar techniques can be used to determine the effect of the crack on the longitudinal dynamic behaviour too. In particular, Rice and Levy [14] demonstrated that a massless spring can be used to represent the compliance due to the crack in both the longitudinal and transverse motion of the beam. Chondros et al. [15] developed a continuous cracked bar vibration theory for longitudinal vibration of rods with an edge-crack and used the Hu–Washizu–Barr variational formulation to obtain the differential equation and the boundary conditions that govern the problem. Moreover, they presented experimental results, showing that they are close to numerical predictions.

For a long time, research in this field has centred on structures with a single fault, although occasionally with two faults [16], while only recently a number of papers have appeared which deal with multi-cracked beams. One of the early articles considering beams with several cracks and solving the related inverse problem was published in 1997 [17], whereas in, Ref. [18] a technique was proposed which lead to very compact determinantal equations for the determination of natural frequencies of beams with an arbitrary number of transverse open cracks. Zheng and Fan [19,20] used a kind of modified Fourier series to compute natural frequencies of Euler–Bernoulli and Timoshenko beams. Khiem and Lien [21] solved the direct problem by using a transfer matrix approach, while Li [22] utilised a properly derived basic solution and a recurrence formula.

Another method for evaluating natural frequencies of a cracked beam is based on the use of the finite element method [23–25]. By employing this approximation technique it is possible to evaluate the dynamic properties of a beam with an arbitrary number of cracks, although this method leads to a system of linear equations and to determinants of high order, thus yielding results with generally less accuracy than continuous models.

Even though the analysis of the transverse dynamic behaviour of multi-cracked beams has been presented in several articles, to the authors' knowledge the longitudinal dynamic behaviour of such structures has not been analyzed.

As a result, the aim of this article is determine the longitudinal dynamic behaviour of bars with several open cracks by extending the method previously proposed by Shifrin and Ruotolo [18] for the prediction of the transverse dynamic behaviour of multi-cracked beams. Some numerical examples complete the article, and comparisons are drawn with corresponding results provided by a transfer matrix approach and by the finite element method.

## 2. Smooth function method

A bar with length $l$ and with $n$ cracks is considered (Fig. 1). It is assumed that cracks are located at points $x_1, x_2, \ldots, x_n$ such that $0 < x_1 < x_2 < \cdots < x_n < l$. Amplitudes of longitudinal displacement

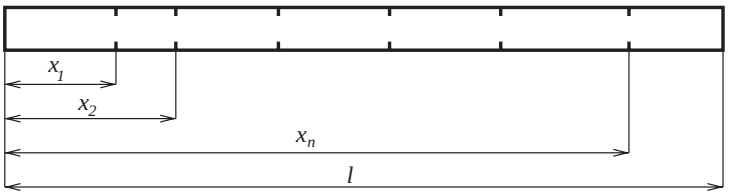


Fig. 1. Multi-cracked bar.

of the beam axis under time-harmonic vibration are denoted by $u_j(x)$ on the interval $x_{j-1}<x<x_j$ where $j=1,2,\ldots,n+1$, $x_0=0$ and $x_{n+1}=l$.

According to the approach proposed in Ref. [6], it is possible to divide the entire bar into $n+1$ bars connected by massless springs representing the $n$ cracks. As a consequence, the equation of harmonic longitudinal oscillations of each bar, assumed with uniform cross section, is

$$EAu_j''(x)+\omega^2\rho Au_j(x)=0, \quad j=1,\ldots,n+1, \ x_{j-1}<x<x_j, \tag{1}$$

where $E$ is Young's modulus, $A$ is the area of the cross section, $\rho$ is the material density, and $\omega$ is a natural circular frequency.

It is possible to introduce two conditions for each connection between two bars which, in correspondence with the location of the crack, impose continuity for the normal force and discontinuity for the longitudinal displacement of the bar in correspondence of the crack.

$$\begin{aligned} &u_j'(x_j)=u_{j+1}'(x_j),\\ &u_{j+1}(x_j)-u_j(x_j)=\Delta_j=EAc_ju_j'(x_j), \quad j=1,2,\ldots,n, \end{aligned} \tag{2}$$

where $c_j$ is the flexibility of the $j$th translational spring which is function of the crack extent and bar width. In order to consider only the effect of the longitudinal vibrations, a double edge crack, symmetrical with respect to the longitudinal axis of the bar has been considered (Fig. 2). In this case, according to the stress intensity factor formulated by Brown in Ref. [26]

$$(K_I)_j=\sigma\sqrt{\pi a_j/2}\,(1.12+0.203\ s_j-1.197\ s_j^2+1.93\ s_j^3), \tag{3}$$

and using the procedure proposed by Rice and Levy [14] $c_j$ can be expressed as

$$c_j=\frac{2h(1-\nu^2)}{EA}\alpha_{tt}(s_j), \tag{4}$$

with $s_j=a_j/h$ where $a_j$ is the depth of the $j$th crack and

$$\begin{aligned} \alpha_{tt}(s_j)=&\,0.7314\ s_j^8-1.0368\ s_j^7+0.5803\ s_j^6+1.2055\ s_j^5\\ &-1.0368\ s_j^4+0.2381\ s_j^3+0.9852\ s_j^2. \end{aligned}$$

Amplitude of displacement $u_j(x)$ can be collected into the function $u(x)$ as follows:

$$u(x)=u_j(x), \quad j=1,\ldots,n+1, \ x_{j-1}<x<x_j,$$

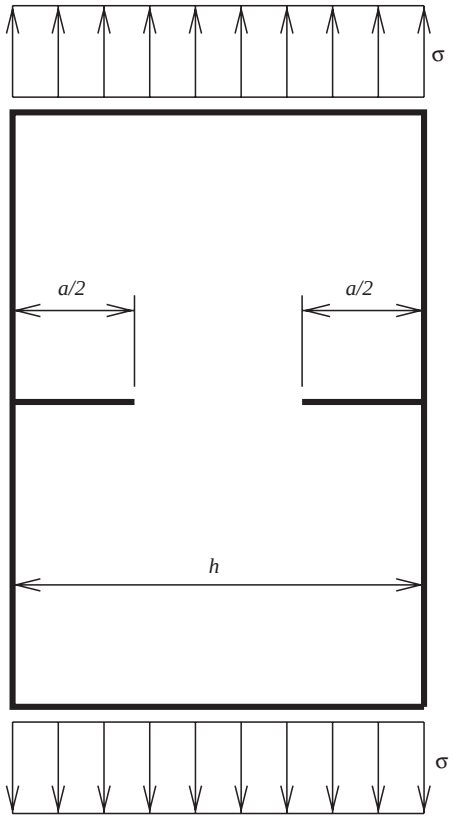


Fig. 2. Double-edge crack.

such that $u(x)$ is able to refer to the displacements of the entire bar axis. Eq. (1) with conditions (2) can be expressed through function $u(x)$ in the following way:

$$u''(x) = -\lambda^2 u(x) + \sum_{j=1}^{n} \Delta_j \delta'(x - x_j), \tag{5}$$

in which $\delta(x)$ is Dirac's delta function and $\lambda^2 = \omega^2 \rho / E$. $\delta'(x)$ appears in Eq. (5) due to the discontinuity of the displacement $u(x)$ at the cracks, as expressed in Eqs. (2).

Furthermore, $u(x)$ is not a smooth function on the interval $[0, l]$ at $x = x_j$. It is possible to introduce a smooth function $u_0(x)$ such as

$$u(x) = u_0(x) + \sum_{j=1}^{n} \Delta_j \mathrm{H}(x - x_j), \tag{6}$$

where $\mathrm{H}(x - x_j)$ is the Heaviside function defined as [27]

$$\mathrm{H}(x - x_j) = \begin{cases} 1 & \text{if } x \geqslant x_j, \\ 0 & \text{if } x < x_j. \end{cases}$$

By introducing Eq. (6) into Eq. (5), and recalling that

$$\delta(x - x_j) = [\mathrm{H}(x - x_j)]',$$

the following equation holds

$$u_0''(x) + \lambda^2 u_0(x) = -\lambda^2 \sum_{j=1}^{n} \Delta_j \mathrm{H}(x - x_j). \tag{7}$$

The general solution of Eq. (7) can be written as

$$u_0(x) = \alpha \cos(\lambda x) + \beta \sin(\lambda x) + \sum_{j=1}^{n} \Delta_j \mathrm{H}(x - x_j)\,[\cos \lambda(x - x_j) - 1], \tag{8}$$

where $\alpha, \beta$, are constants. By differentiating the previous function once it is possible to obtain the expression for $u_0'(x)$ at the cracks positions $x_i$:

$$u_0'(x_i) = -\alpha\lambda \sin(\lambda x_i) + \beta\lambda \cos(\lambda x_i) + \sum_{j=1}^{n} \Delta_j N_{ij}, \tag{9}$$

where

$$N_{ij}(\lambda) = \delta(x_i - x_j)\,[\cos \lambda(x_i - x_j) - 1] - \mathrm{H}(x_i - x_j) \sin \lambda(x_i - x_j)\lambda, \tag{10}$$

where

$$\begin{aligned} &N_{ij}(\lambda) = 0, \quad x_i \leqslant x_j, \\ &N_{ij}(\lambda) = -\lambda \sin \lambda(x - x_j), \quad x_i > x_j. \end{aligned} \tag{11}$$

Using Eqs. (9), (10) and as

$$\lim_{x \to x_i} u'(x) = u_0'(x_i), \quad i = 1, 2, \ldots, n, \tag{12}$$

the last of conditions (2), i.e., $\Delta_i = EAc_i u'(x_i)$, can be expressed as

$$\Delta_i = EA\lambda c_i[-\alpha \sin(\lambda x_i) + \beta \cos(\lambda x_i) - \sum_{j=1}^{n} \Delta_j \sin \lambda(x_i - x_j)], \quad i = 1, \ldots, n. \tag{13}$$

It is necessary to point out that Eq. (13) are valid for all kinds of end conditions of the bar under analysis. Furthermore, Eq. (13) are a system of $n$ linear equations with $n + 2$ unknowns (constants $\alpha$, $\beta$, and $\Delta_i$). In order to solve the system it is necessary to introduce other two equations, which are simply obtained by taking into account the end conditions for the bar under analysis.

## 3. Transfer matrix method

In this section the method of transfer matrix, used by Khiem and Lien [21] for calculating the natural frequencies of a multi-cracked beam in bending vibration, has been extended to determine the natural frequencies of a bar with different end conditions.

For the $j$th segment $[x_{j-1}, x_j]$, let

$$\{\mathbf{Z}(x_k)\}_j = \left\{ \begin{array}{c} u_j(x_k) \\ EAu'_j(x_k) \end{array} \right\}, \tag{14}$$

where $k = (j-1)$ or $k = j$ if the left or the right end is considered, respectively. The general solution for the $j$th segment of Eq. (1) is

$$u_j(x) = C_{1,j} \cos \lambda(x - x_{j-1}) + C_{2,j} \sin \lambda(x - x_{j-1}). \tag{15}$$

The coefficients $C_{1,j}$ and $C_{2,j}$ can be obtained by evaluating function $u_j(x)$ and its derivative at $x = x_{j-1}$

$$C_{1,j} = u_j(x_{j-1}) = \mathbf{Z}(x_{j-1})_{j,1} \quad C_{2,j} = \frac{u'_j(x_{j-1})}{\lambda} = \frac{\mathbf{Z}(x_{j-1})_{j,2}}{\lambda EA}. \tag{16}$$

Substituting Eq. (16) in Eq. (15) the following expression is obtained

$$u_j(x) = \mathbf{Z}(x_{j-1})_{j,1} \cos \lambda(x - x_{j-1}) + \frac{\mathbf{Z}(x_{j-1})_{j,2}}{\lambda EA} \sin \lambda(x - x_{j-1}). \tag{17}$$

Using Eq. (17) the relationship between $\{\mathbf{Z}(x_j)\}_j$ and $\{\mathbf{Z}(x_{j-1})\}_j$, respectively, at the right and at the left of the segment $j$ of length $l_j = x_j - x_{j-1}$, can be written

$$\begin{aligned} \mathbf{Z}(x_j)_{j,1} &= \mathbf{Z}(x_{j-1})_{j,1} \cos \lambda l_j + \frac{\mathbf{Z}(x_{j-1})_{j,2}}{\lambda EA} \sin \lambda l_j, \\ \mathbf{Z}(x_j)_{j,2} &= -\mathbf{Z}(x_{j-1})_{j,1} \lambda EA \sin \lambda l_j + \mathbf{Z}(x_{j-1})_{j,2} \cos \lambda l_j, \end{aligned} \tag{18}$$

and, in matrix form

$$\{\mathbf{Z}(x_j)\}_j = [\mathbf{T}]_j \{\mathbf{Z}(x_{j-1})\}_j, \tag{19}$$

with

$$[\mathbf{T}]_j = \begin{bmatrix} \cos \lambda l_j & \sin \lambda l_j / \lambda EA \\ -\lambda EA \sin \lambda l_j & \cos \lambda l_j \end{bmatrix}. \tag{20}$$

In correspondence with the $j$th crack, the relationship between $\{\mathbf{Z}(x_j)\}_{j+1}$ and $\{\mathbf{Z}(x_j)\}_j$, respectively, at the right and at the left of the crack is

$$\{\mathbf{Z}(x_j)\}_{j+1} = [\mathbf{J}]_j \{\mathbf{Z}(x_j)\}_j, \tag{21}$$

where

$$[\mathbf{J}]_j = \begin{bmatrix} 1 & c_j \\ 0 & 1 \end{bmatrix}, \tag{22}$$

with $c_j$ already expressed in Eq. (4).

Introducing expression (19) into (21) the following is obtained

$$\{\mathbf{Z}(x_j)\}_{j+1} = [\mathbf{J}]_j [\mathbf{T}]_j \{\mathbf{Z}(x_{j-1})\}_j = [\mathbf{Q}]_j \{\mathbf{Z}(x_{j-1})\}_j, \tag{23}$$

where

$$
\begin{aligned}
Q_{11,j} &= \cos \lambda l_j - c_j \lambda EA \sin \lambda l_j \\
Q_{12,j} &= \sin \lambda l_j / \lambda EA + c_j \cos \lambda l_j \\
Q_{21,j} &= -\lambda EA \sin \lambda l_j \\
Q_{22,j} &= \cos \lambda l_j.
\end{aligned} \tag{24}
$$

Consequently, variables at the right end of the bar can be expressed as a function of those at the left end:

$$
\{\mathbf{Z}(x_{n+1})\}_{n+1} = [\mathbf{T}]_{n+1}[\mathbf{Q}]_n[\mathbf{Q}]_{n-1} \ldots [\mathbf{Q}]_1 \{\mathbf{Z}(x_0)\}_1 = [\mathbf{Q}]\{\mathbf{Z}(x_0)\}_1. \tag{25}
$$

The matrix $[\mathbf{Q}]$ depends on the natural frequencies of the bar, on the position of the cracks $\{\mathbf{x}\} = \lfloor x_1, x_2, \ldots, x_n \rfloor^{\mathrm{T}}$ and on the extents of the cracks $\{\mathbf{c}\} = \lfloor c_1, c_2, \ldots, c_n \rfloor^{\mathrm{T}}$.

The boundary conditions can be expressed in the following way:

$$
\begin{aligned}
[\mathbf{B}_1^0 \mathbf{B}_2^0] \begin{Bmatrix} u_1(x_0 = 0) \\ EAu_1'(x_0 = 0) \end{Bmatrix} &= 0, \\
[\mathbf{B}_1^l \mathbf{B}_2^l] \begin{Bmatrix} u_{n+1}(x_{n+1} = l) \\ EAu_{n+1}'(x_{n+1} = l) \end{Bmatrix} &= 0,
\end{aligned} \tag{26}
$$

or in a more compact form as:

$$
\begin{aligned}
\{\mathbf{B}^0\}^{\mathrm{T}} \{\mathbf{Z}(x_0)\}_1 &= 0, \\
\{\mathbf{B}^l\}^{\mathrm{T}} \{\mathbf{Z}(x_{n+1})\}_{n+1} = \{\mathbf{B}^l\}^{\mathrm{T}} [\mathbf{Q}] \{\mathbf{Z}(x_0)\}_1 &= 0,
\end{aligned} \tag{27}
$$

and can be combined together as

$$
[\mathbf{A}]\{\mathbf{Z}(x_0)\}_1 = \{\mathbf{0}\}, \tag{28}
$$

with

$$
[\mathbf{A}] = \begin{bmatrix} \{\mathbf{B}^0\}^{\mathrm{T}} \\ \{\mathbf{B}^l\}^{\mathrm{T}} [\mathbf{Q}] \end{bmatrix} = \begin{bmatrix} B_1^0 & B_2^0 \\ \sum_{j=1}^{2} B_j^l Q_{j1} & \sum_{j=1}^{2} B_j^l Q_{j2} \end{bmatrix}. \tag{29}
$$

In order to determine the natural frequencies of the bar, the following equation must be solved:

$$
\det[\mathbf{A}(\omega, \{\mathbf{x}\}, \{\mathbf{c}\})] = \mathbf{B}_1^0(\mathbf{B}_1^l \mathbf{Q}_{12} + \mathbf{B}_2^l \mathbf{Q}_{22}) - \mathbf{B}_2^0(\mathbf{B}_1^l \mathbf{Q}_{11} + \mathbf{B}_2^l \mathbf{Q}_{21}) = 0. \tag{30}
$$

For the following boundary conditions Eq. (30) becomes

$$
\begin{aligned}
&\text{free}-\text{free} \;\; \mathbf{B}_1^0 = \mathbf{B}_1^l = \mathbf{0} \quad \det[\mathbf{A}] = -\mathbf{B}_2^0 \mathbf{B}_2^l \mathbf{Q}_{21} = \mathbf{Q}_{21} = \mathbf{0}, \\
&\text{fixed}-\text{free} \;\; \mathbf{B}_2^0 = \mathbf{B}_1^l = \mathbf{0} \quad \det[\mathbf{A}] = \mathbf{B}_1^0 \mathbf{B}_2^l \mathbf{Q}_{22} = \mathbf{Q}_{22} = \mathbf{0}, \\
&\text{fixed}-\text{fixed} \;\; \mathbf{B}_2^0 = \mathbf{B}_2^l = \mathbf{0} \quad \det[\mathbf{A}] = \mathbf{B}_1^0 \mathbf{B}_1^l \mathbf{Q}_{12} = \mathbf{Q}_{12} = \mathbf{0}.
\end{aligned} \tag{31}
$$

## 4. Results

### 4.1. Numerical results

In order to validate the procedures proposed in this paper, the dynamic behaviour of a bar with three cracks has been simulated. The results are compared with those obtained using a finite element model with ten elements; the cracked element is described in the Appendix.

The bar under analysis has the following mechanical properties: Young's modulus $E = 2.1 \times 10^{11}$ N/m$^2$, material density $\rho = 7800$ kg/m$^2$, the Poisson's ratio $v = 0.3$ and rectangular cross-section with width $b = 0.02$ m and height $h = 0.02$ m. The first four natural frequencies for both fixed–free and free–free bar, for the undamaged case, are listed in Table 1, allowing comparison of the results predicted by the continuous model with the finite element method.

The bar with a fixed end has a first crack at position $x_1 = 0.04$ m and depth $a_1 = 6$ mm, a second crack at position $x_2 = 0.12$ m and depth $a_2 = 4$ mm. A third crack with a variable position ranging from 0.2 to 0.8 m (distance calculated from the fixed end) and a relative depth $s_3 = a_3/h$ of 0.1, 0.2 and 0.3 was introduced.

The ratio between the first four natural frequencies of cracked and uncracked bar is shown in Figs. 3–6. Focusing the attention on the first two natural frequency ratios, shown in Figs. 3 and 4, a very good agreement can be seen among the results obtained by using the three models. For the third and the fourth natural frequency the results, in terms of frequency ratio, obtained with the transfer matrix method are closer to the results obtained with the finite element model, even though there are relatively large differences in the predicted natural frequencies for undamaged bars, as already shown in Table 1. However, even in these cases discrepancies are negligible, as is also demonstrated in Table 2, where the maximum relative difference for natural frequencies predicted using the method described in Section 2 and the transfer matrix method are listed for the case of the deepest crack. This table shows that relative differences between the predictions are lower than 0.04%.

Figs. 7–10 show the same kind of results for the bar in free–free conditions.

In order to determine the accuracy of the results predicted by the finite element method, a convergence analysis has been performed, by varying the number of elements discretising the structure. For this purpose a fixed–free bar with the same mechanical and geometrical characteristics of the previous examples has been considered. The bar has a single crack of relative depth $s = 0.3$ located in the middle-span. Fig. 11 shows the trend of the error on the non-dimensional reduction of the first four longitudinal natural frequencies with respect to the

Table 1
Natural frequencies for the undamaged bars evaluated using the continuous model and FEM

| | Fixed–free bar | | Free–free bar | |
|---|---|---|---|---|
| $f_n$ (Hz) | Continuous | FEM | Continuous | FEM |
| 1 | 1621 | 1623 | 3243 | 3256 |
| 2 | 4864 | 4910 | 6486 | 6593 |
| 3 | 8107 | 8317 | 9729 | 10 092 |
| 4 | 11 350 | 11 927 | 12 972 | 13 832 |

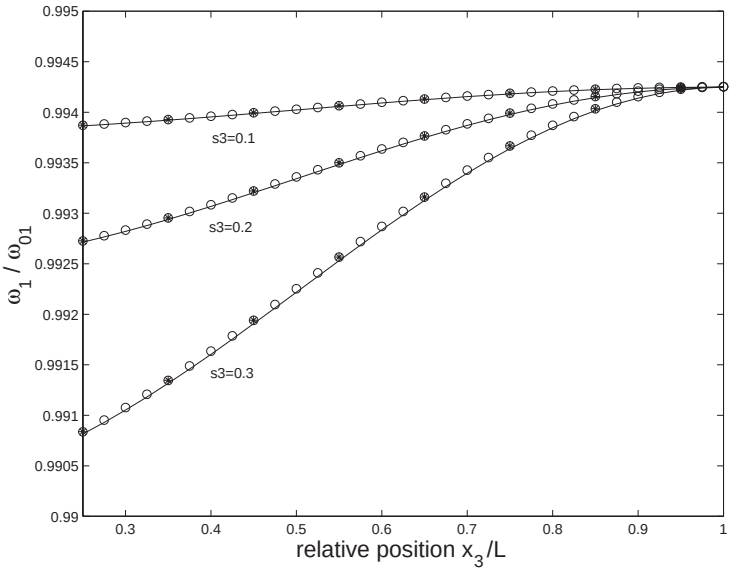


Fig. 3. Effect of the third crack on the first natural frequency for the fixed–free bar (—, smooth function method; ◦, transfer matrix method; ∗, FEM).

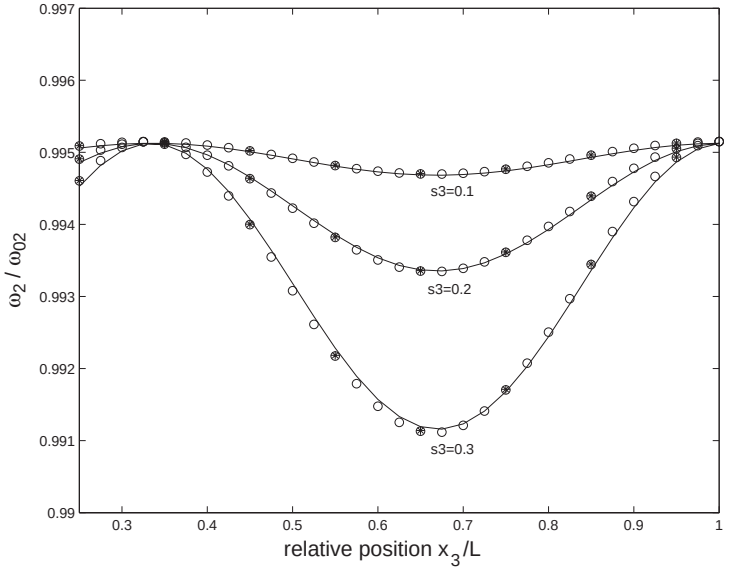


Fig. 4. Effect of the third crack on the second natural frequency for the fixed–free bar (—, smooth function method; ◦, transfer matrix method; ∗, FEM).

asymptotic value:

$$\varepsilon_k^{(i)} = \frac{(\Delta\omega_i/\omega_i)_k}{(\Delta\omega_i/\omega_i)_{41}} - 1, \tag{32}$$

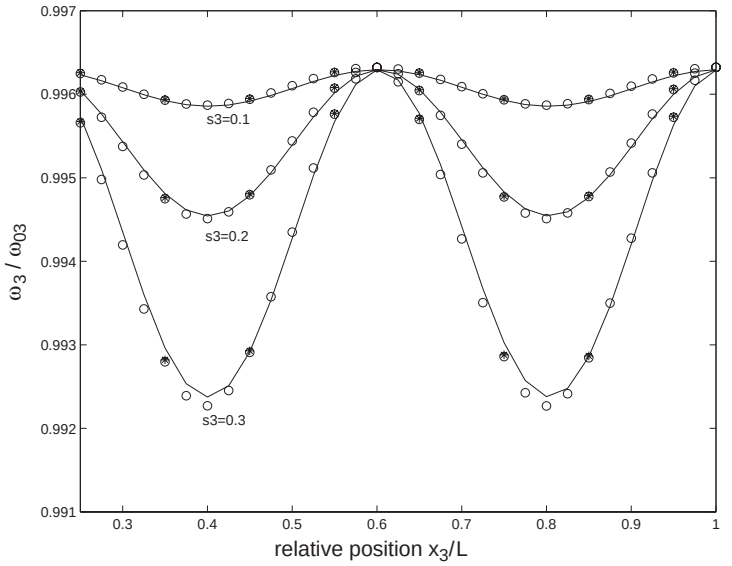


Fig. 5. Effect of the third crack on the third natural frequency for the fixed–free bar (—, smooth function method; ◦, transfer matrix method; ∗, FEM).

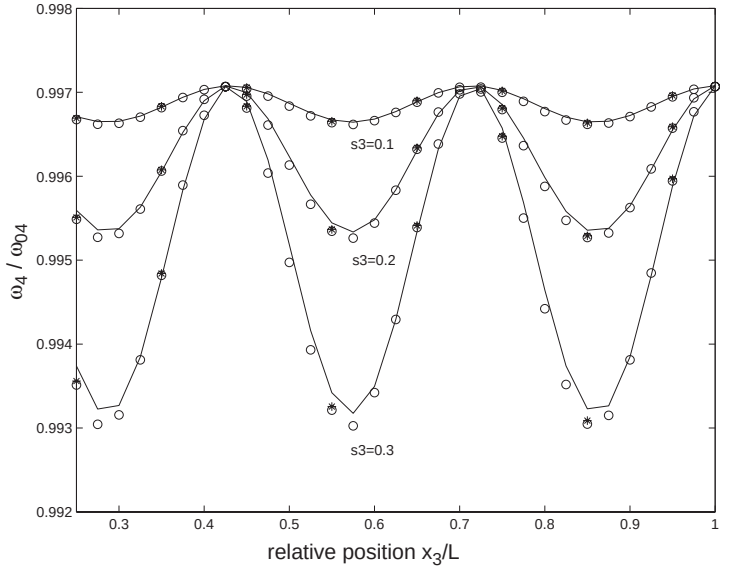


Fig. 6. Effect of the third crack on the fourth natural frequency for the fixed–free bar (—, smooth function method; ◦, transfer matrix method; ∗, FEM).

where 41 is the maximum number of elements considered to subdivide the bar under analysis. The figure indicates that the maximum error has magnitude of 0.01% even for a rather coarse mesh with only 5 elements. This is an interesting result, demonstrating that although, in general, a relatively high number of elements is necessary to predict the eigenfrequencies (i.e., $\omega_n$) of the

Table 2
Maximum relative difference between natural frequencies evaluated using the smooth function method ($f_i$) and the transfer matrix method ($f_{i,TM}$)

| $i$ | $f_i$ (Hz) | $\lvert f_i - f_{i,TM}\rvert / f_i$ (%) | Position ($x_3/l$) |
|---|---|---|---|
| *Fixed–free bar* | | | |
| 1 | 1609.4 | 0.0036 | 0.550 |
| 2 | 4826.9 | 0.0111 | 0.550 |
| 3 | 8055.5 | 0.0172 | 0.325 |
| 4 | 11284.0 | 0.0231 | 0.525 |
| *Free–free bar* | | | |
| 1 | 3228.4 | 0.0038 | 0.550 |
| 2 | 6450.9 | 0.0138 | 0.800 |
| 3 | 9669.9 | 0.0260 | 0.550 |
| 4 | 12893.0 | 0.0362 | 0.925 |

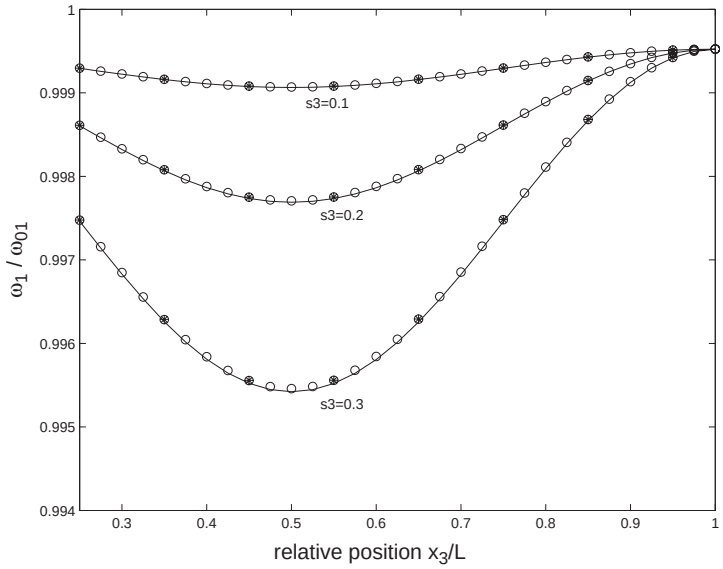


Fig. 7. Effect of the third crack on the first natural frequency for the free–free bar (—, smooth function method; ◦, transfer matrix method; ∗, FEM).

structure under analysis with a sufficient precision, a coarse mesh is able to predict accurately the sensitivity (i.e., $\Delta\omega_n/\omega_n$) of natural frequencies to the presence of a crack.

### 4.2. Comparison with experimental results

Fig. 12 shows the comparison between predictions obtained by using several mathematical models with experimental results presented in Ref. [15] by Chondros et al. The bar under analysis

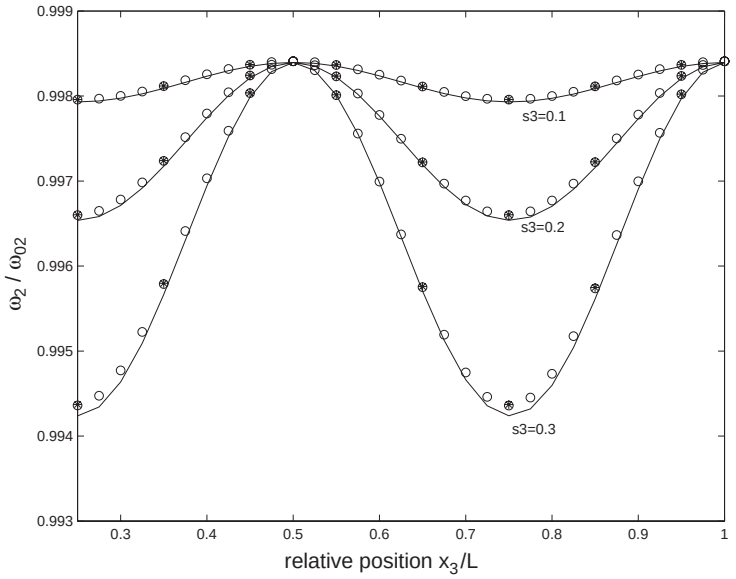


Fig. 8. Effect of the third crack on the second natural frequency for the free–free bar (—, smooth function method; ◦, transfer matrix method; ∗, FEM).

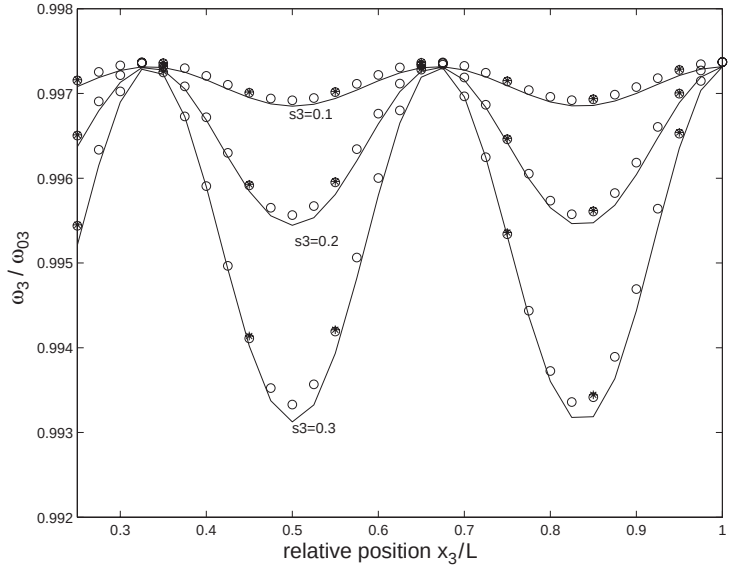


Fig. 9. Effect of the third crack on the third natural frequency for the free–free bar (—, smooth function method; ◦, transfer matrix method; ∗, FEM).

has the following properties: cross-section with width of 6 mm and height of 23 mm, length of 235 mm, Young's modulus $E = 7.2 \times 10^{10}$ N/m$^2$ and material density of 2800 kg/m$^3$. As described in Ref. [15], a single crack propagated perpendicular to the longitudinal axis at

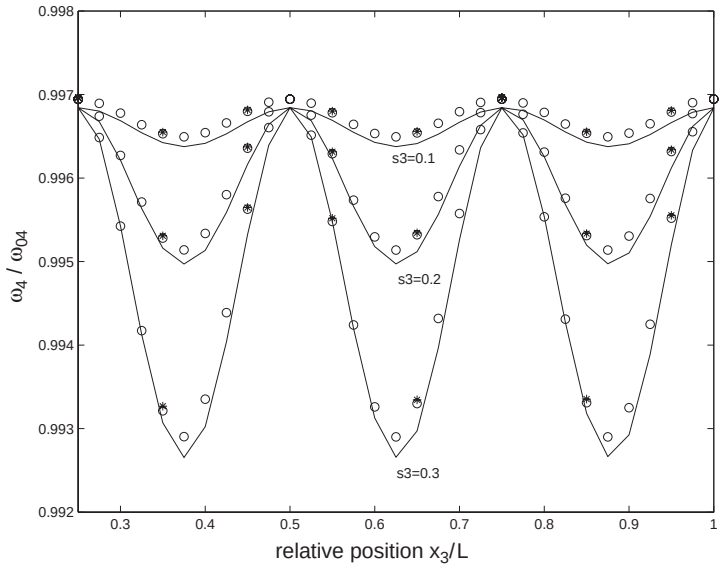


Fig. 10. Effect of the third crack on the fourth natural frequency for the free–free bar (—, smooth function method; ◦, transfer matrix method; ∗, FEM).

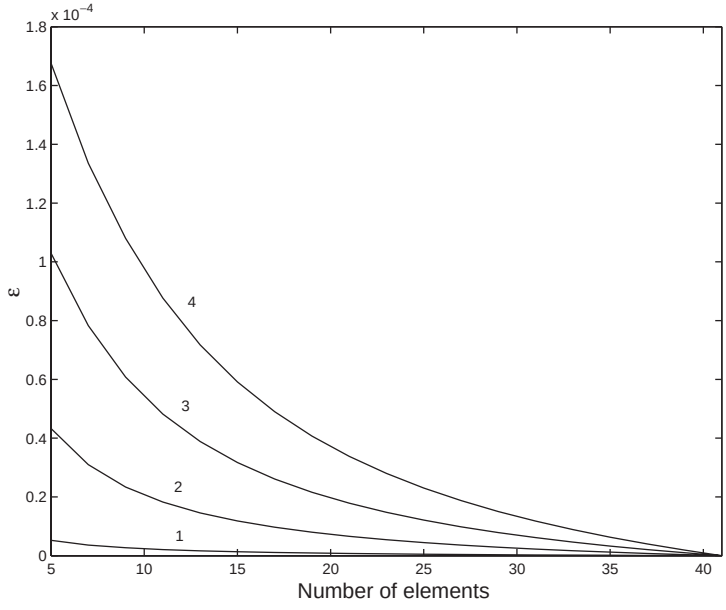


Fig. 11. Error in non-dimensional reduction for the first four natural frequencies versus the number of elements of the mesh.

mid-span and the fundamental longitudinal natural frequency was estimated by hammer testing the free–free bar. The simulations were performed considering the stress intensity factor relative to a one-edge crack used in Ref. [15]. In Fig. 12 the relative reduction of the first longitudinal natural

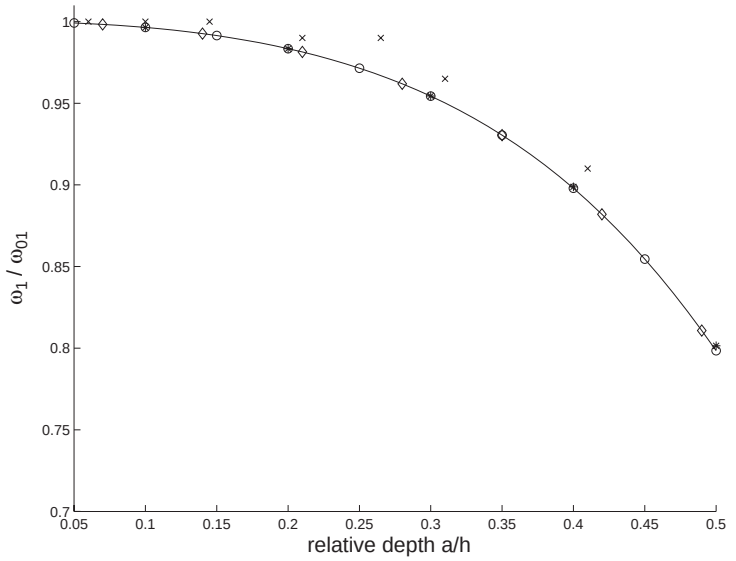


Fig. 12. Comparison with results published in [15] (—, smooth function method; ◦, transfer matrix method; ∗, FEM; ◇, lumped bar model [15]; $x$, experimental data).

frequency of the bar versus the relative depth $a/h$ of the crack is shown. This figure shows extremely good agreement among predictions provided by the various mathematical models and a very good correlation with experimental results, even though all the mathematical models predict a reduction higher than that estimated during the vibration tests.

## 5. Conclusions

In this paper natural frequencies of a cracked bar are evaluated by representing cracks as massless springs and considering a continuous mathematical model of the bar in longitudinal vibration. Two approaches have been used: the smooth function method and the transfer matrix method. In both cases it is possible to determine the eigenfrequencies of the bar from the roots of a determinant that can be written in a concise manner for an arbitrary number of cracks $n$, enabling the times of computation to be reduced.

In the case of the smooth function method the determinant of a $(n+2)\times(n+2)$ dimension matrix, is calculated, while in the case of the transfer function method the natural frequencies of the cracked bar are determined by determinant calculation of a $2\times 2$ dimension matrix, although this matrix is obtained performing $n$ multiplications of $n+1$ matrices; alternatively the determinant of a $(2n+2)\times(2n+2)$ dimension matrix would be computed, when applying the classical procedure developed in [6,16].

Finally a comparison of results obtained using the two methods based on a continuous model and the finite element method shows a very good agreement giving validity to the procedures proposed.

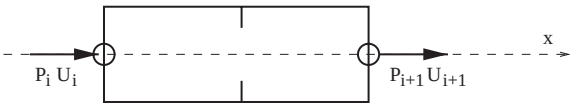


Fig. 13. Cracked finite element.

## Acknowledgements

The authors would like to thank Dr. Pietro Cornetti for the useful discussions.

## Appendix. Finite element model of the cracked bar

The mathematical model used for the bar with a transverse on-edge not propagating fatigue crack is based on the finite element model proposed in Ref. [23].

A two node finite bar element with one degree of freedom per node with a transverse on-edge not propagating open crack is shown in Fig. 13. The stiffness matrix $[\mathbf{K}_d]_e$ of this element has been calculated by means of the relationship [24]

$$[\mathbf{K}_d]_e = \frac{1}{(c_0 + c_1)} \{\mathbf{T}\}\{\mathbf{T}\}^{\mathrm{T}}, \tag{A.1}$$

where $\mathbf{T} = \{-1, 1\}^{\mathrm{T}}$ is a transformation vector, $c_0 = L/EA$ is the flexibility of the non-cracked element [28] and $c_1$ is the additional flexibility of the element due to crack already defined in Eq. (4).

It is supposed that the crack does not affect the mass matrix [**M**]. Therefore for a single element,

$$[\mathbf{M}]_e = \frac{\rho AL}{6} \begin{bmatrix} 2 & 1 \\ 1 & 2 \end{bmatrix}. \tag{A.2}$$

## References

[1] S.W. Doebling, C.R. Farrar, M.B. Prime, D.W. Shevitz, Damage identification and health monitoring of structural and mechanical systems from changes in their vibration characteristics: a literature review, Report No. LA-13070-MS, Los Alamos National Laboratory, Los Alamos, NM, 1996.

[2] A.D. Dimarogonas, Vibration of cracked structures: a state of the art review, *Engineering Fracture Mechanics* 55 (5) (1996) 831–857.

[3] M.M. Yuen, A numerical study of the eigenparameters of a damaged cantilever, *Journal of Sound and Vibration* 103 (3) (1985) 301–310.

[4] A.D. Dimarogonas, *Vibration Engineering*, West Publishers, St. Paul, MN, 1976.

[5] T.G. Chondros, A.D. Dimarogonas, Identification of cracks in welded joints of complex structures, *Journal of Sound and Vibration* 69 (4) (1980) 531–538.

[6] P.F. Rizos, N. Aspragatos, A.D. Dimarogonas, Identification of crack location and magnitude in a cantilever beam from the vibration modes, *Journal of Sound and Vibration* 138 (3) (1990) 381–388.

[7] R. Ruotolo, C. Surace, C. Mares, Theoretical and experimental study of the dynamic behaviour of a double-cracked beam, *Proceedings of the 14th International Modal Analysis Conference*, 1996, pp. 1560–1564.

[8] R.Y. Liang, J. Hu, F. Choy, Theoretical study of crack-induced eigenfrequency changes on beam structures, *Journal of Engineering Mechanics* 118 (2) (1992) 384–396.
[9] R.Y. Liang, J. Hu, F. Choy, Quantitative NDE techniques for assessing damages in beam structures, *Journal of Engineering Mechanics* 118 (7) (1992) 1468–1487.
[10] R.Y. Liang, F. Choy, J. Hu, Detection of cracks in beam structures using measurements of natural frequencies, *Journal of the Franklin Institute* 328 (4) (1991) 505–518.
[11] J. Hu, R.Y. Liang, An integrated approach to detection of cracks using vibration characteristics, *Journal of the Franklin Institute* 330 (5) (1993) 841–853.
[12] A. Morassi, Crack induced changes in eigenfrequencies of beam structures, *Journal of Engineering Mechanics* 119 (9) (1993) 1768–1803.
[13] S. Christides, A.D.S. Barr, One-dimensional theory of cracked Euler–Bernoulli beams, *International Journal of Mechanical Science* 26 (1984) 639–648.
[14] J.R. Rice, N. Levy, The part through surface crack in an elastic plate, *Journal of Applied Mechanics* 39 (1972) 185–194.
[15] T.G. Chondros, A.D. Dimarogonas, J. Yao, Longitudinal vibration of a continuous cracked bar, *Engineering Fracture Mechanics* 61 (1998) 593–606.
[16] W.M. Ostachowicz, M. Krawczuk, Analysis of the effect of cracks on the natural frequencies of a cantilever beam, *Journal of Sound and Vibration* 150 (2) (1991) 191–201.
[17] R. Ruotolo, C. Surace, Damage assessment of multiple cracked beams: numerical results and experimental validation, *Journal of Sound and Vibration* 206 (4) (1997) 567–588.
[18] E. Shifrin, R. Ruotolo, Natural frequencies of a beam with an arbitrary number of cracks, *Journal of Sound and Vibration* 222 (3) (1999) 409–423.
[19] D.Y. Zheng, S.C. Fan, Natural frequencies of a non-uniform beam with multiple cracks via modified fourier series, *Journal of Sound and Vibration* 242 (4) (2001) 701–717.
[20] D.Y. Zheng, S.C. Fan, Natural frequency changes of a cracked Timoshenko beam by modified fourier series, *Journal of Sound and Vibration* 246 (2) (2001) 297–317.
[21] N.T. Khiem, T.V. Lien, A simplified method for natural frequency analysis of a multiple cracked beam, *Journal of Sound and Vibration* 245 (4) (2001) 737–751.
[22] Q.S. Li, Free vibration analysis of non-uniform beams with an arbitrary number of cracks and concentrated masses, *Journal of Sound and Vibration* 252 (3) (2002) 509–525.
[23] G. Gounaris, A.D. Dimarogonas, A finite element of a cracked prismatic beam for a structural analysis, *Computer and Structures* 28 (3) (1988) 309–313.
[24] G.-L. Qian, S.-N. Gu, J.-S. Jiang, Dynamic behaviour and crack detection of a beam with a crack, *Journal of Sound and Vibration* 138 (2) (1990) 233–243.
[25] B.S. Haisty, W.T. Springer, A general beam element for use in damage assessment of complex structures, *Journal of Vibration, Acoustics, Stress and Reliability in Design* 110 (1988) 389–394.
[26] H. Tada, P.C. Paris, G.R. Irwin, *The Stress Analysis of Cracks Handbook*, Paris Productions, St. Louis, MO, 1985.
[27] J.W. Dettman, *Mathematical Methods in Physics and Engineering*, McGraw-Hill, New York, 1969.
[28] J.S. Przemieniecki, *Theory and Matrix Structural Analysis*, Dover Publications, New York, 1985.